



The HipAB Toxin–Antitoxin System Stabilizes a Composite Genomic Island in *Shewanella putrefaciens* CN-32

Yi Zhao¹, Weiquan Wang^{2,3,4}, Jianyun Yao^{2,3}, Xiaoxue Wang^{2,3,4}, Dong Liu^{1*} and Pengxia Wang^{2,3,4*}

¹College of Life Sciences, Hebei Normal University, Shijiazhuang, China, ²Key Laboratory of Tropical Marine Bio-resources and Ecology, Guangdong Key Laboratory of Marine Materia Medica, Innovation Academy of South China Sea Ecology and Environmental Engineering, South China Sea Institute of Oceanology, Chinese Academy of Sciences, Guangzhou, China, ³Southern Marine Science and Engineering Guangdong Laboratory (Guangzhou), Guangzhou, China, ⁴University of Chinese Academy of Sciences, Beijing, China

OPEN ACCESS

Edited by:

Daniel Yero,
Universidad Autónoma de Barcelona,
Spain

Reviewed by:

Alberto J. Martín-Rodríguez,
Karolinska Institutet (KI), Sweden
Frédéric Goormaghtigh,
University of Basel, Switzerland

*Correspondence:

Dong Liu
pqw1234@163.com
orcid.org/0000-0003-1546-8215
Pengxia Wang
wangpengxia@scsio.ac.cn
orcid.org/0000-0002-1267-6118

Specialty section:

This article was submitted to
Evolutionary and Genomic
Microbiology,
a section of the journal
Frontiers in Microbiology

Received: 20 January 2022

Accepted: 24 February 2022

Published: 21 March 2022

Citation:

Zhao Y, Wang W, Yao J, Wang X,
Liu D and Wang P (2022) The HipAB
Toxin–Antitoxin System Stabilizes a
Composite Genomic Island in
Shewanella putrefaciens CN-32.
Front. Microbiol. 13:858857.
doi: 10.3389/fmicb.2022.858857

Composite genomic islands (GIs) are useful models for studying GI evolution if they can revert into the previous components. In this study, CGI48—a 48,135-bp native composite GI that carries GI21, whose homologies specifically integrated in the conserved *yicC* gene—were identified in *Shewanella putrefaciens* CN-32. CGI48 was integrated into the *tRNA^{Trp}* gene, which is a conserved gene locus for the integration of genomic islands in *Shewanella*. Upon expressing integrase and excisionase, CGI48 and GI21 are excised from chromosomes *via* site-specific recombination. The shorter attachment sites of GI21 facilitated the capture of GI21 into CGI48. Moreover, GI21 encodes a functional HipAB toxin–antitoxin system, thus contributing to the maintenance of CGI48 in the host bacteria. This study provides new insights into GI evolution by performing the excision process of the inserting GI and improves our understanding of the maintenance mechanisms of composite GI.

Keywords: *Shewanella putrefaciens*, mobile genetic element, stability, genomic island, toxin–antitoxin

INTRODUCTION

Genomic islands (GIs) are discrete DNA segments acquired by horizontal transfer, and they always differ among closely related strains. GIs vary in size from a few to several kilobase pairs and have a mosaic structure that evolves by gene acquisition and loss (Bellanger et al., 2014). Horizontal transfer of GIs can be advantageous for the host, influencing traits, such as pathogenicity, symbiosis, metabolism, phage resistance, and fitness (Dobrindt et al., 2004; Bellanger et al., 2014). Therefore, an understanding of GI evolution is critical for understanding the acquisition of these important adaptive traits.

Composite GI formation is a special type of GI evolution in which one mobile genetic element (MGE) is inserted within another or into the attachment sites of a resident GI (tandem accretion; Bellanger et al., 2014). Many composite GIs have been found through genome comparison (Bellanger et al., 2014), such as the SGI1 variant SGI1-B2 from *Proteus mirabilis*

(Lei et al., 2015), ICES $t1$ and CIME302 elements of *Streptococcus thermophilus* (Burrus et al., 2000), and ICE6013 from *Staphylococcus aureus* (Smyth and Robinson, 2009). The native composite GIs have likely undergone some complicated recombination events; therefore, it is difficult to reconstruct their precise evolutionary history. To date, the formation processes of a few native composite GIs have been determined, such as the tripartite integrative and conjugative element (ICE) assembled through recombination from two GIs with integrases and one ICE without an integrase in *Mesorhizobium ciceri* (Haskett et al., 2016), the tandem structure of GI $_{prfC}$ inserting in the integration site for SXT/R391 ICEs in *Pseudoalteromonas* sp. SCSIO 11900 in our previous study (Wang et al., 2017). Native composite islands that can replicate their evolutionary processes under laboratory conditions would be especially useful for improving our understanding of GI evolution. Interestingly, how composite GIs maintain structural stability should also be explored.

Toxin–antitoxin (TA) systems were originally discovered on conjugative plasmids and participated in their stable maintenance in host bacteria (Ogura and Hiraga, 1983; Roberts et al., 1994). The TA system consists of two neighboring genes, encoding a stable toxin killing the cell or inhibiting cell growth and an unstable antitoxin that masks its toxicity (Wang et al., 2021). A proposed mechanism post-segregationally killing (PSK) was established based on the differential stability of the antitoxin and toxin components. In PSK, plasmid-loss cells do not survive, so the plasmid is maintained in the population (Jurenas et al., 2022). Currently, TA systems have also been found to be ubiquitous in bacterial chromosomes and have been suggested to contribute to the maintenance of integrative MGEs. For example, the MosAT system promotes the maintenance of SXT family ICE carried by some *Vibrio cholerae* strains (Wozniak and Waldor, 2009); the Par $_{ESc}$ /Cop $_{A_{SO}}$ system stabilizes prophage CP4So in *Shewanella oneidensis* (Yao et al., 2018). Whether the TA system also participates in the maintenance of composite GI is unknown. In this study, a new composite island CGI48 was identified and characterized from *Shewanella putrefaciens* CN32 using genome comparison and excision assay. It evolved by inserting a 21-kb genomic island GI21 into the internal region of CGI48. We further show that GI21 carries a functional HipAB toxin–antitoxin system and contributes to the maintenance of CGI48 in the bacterial host.

MATERIALS AND METHODS

Bacterial Strains and Growth Conditions

The bacterial strains and plasmids used in this study are listed in Table 1. *Shewanella* was grown in LB medium at 30°C. *Escherichia coli* WM3064 was grown in LB medium containing 0.3 mM 2,6-diamino-pimelic acid (DAP) at 37°C. Chloramphenicol (Cm; 30 $\mu\text{g ml}^{-1}$), kanamycin (50 $\mu\text{g ml}^{-1}$), and ampicillin (100 $\mu\text{g ml}^{-1}$) were used in *E. coli*, and chloramphenicol (10 $\mu\text{g ml}^{-1}$) was used in *Shewanella*. Isopropyl- β -D-thiogalactopyranoside (IPTG) was used as an inducer.

TABLE 1 | Strains and plasmids used in this study.

Strains/plasmids	Description ^a	Reference
<i>Shewanella putrefaciens</i> strains		
CN32	<i>Shewanella putrefaciens</i> CN32 wild type	Lab stock
Δ hipAB	Deletion of hipAB genes in CN32	This study
Δ GI21	Deletion of GI21 in CN32	This study
Δ CGI48	Deletion of CGI48 in CN32	This study
CN32 P $_{int}$::lacZ	Integration of plasmid pHGI01 in <i>int</i> promoter to monitor the CGI48 and GI21 loss in CN32 wild type	This study
Δ hipAB P $_{int}$::lacZ	Integration of plasmid pHGI01 in <i>int</i> promoter to monitor the CGI48 and GI21 loss in strain Δ hipAB	This study
W3-18-1	<i>Shewanella putrefaciens</i> W3-18-1 wild type	Caro-Quintero et al., 2011
ANA3	<i>Shewanella</i> sp. ANA-3 wild type	Lab stock
<i>Escherichia coli</i> strains		
WM3064	RP4(tra) in chromosome, DAP $^{-}$, 37°C	Dehio and Meyer, 1997
K-12 BW25113	lacI q rrmB $_{T14}$ Δ lacZ $_{YJ16}$ hsdR514 Δ araBAD $_{AH33}$ Δ raBAD $_{LD78}$	Baba et al., 2006
Plasmids		
pCA24N	Cm R ; lacI q , IPTG inducible expression plasmid in <i>E. coli</i>	Kitagawa et al., 2005
pHipA	Cm R ; lacI q , P $_{T5-lac}$::hipA	This study
pHipB	Cm R ; lacI q , P $_{T5-lac}$::hipB	This study
pHipAB	Cm R ; lacI q , P $_{T5-lac}$::hipA-hipB	This study
pHGECm	Cm R ; Kan R ; IPTG inducible expression plasmid	Wang et al., 2017
pMD19-T	Amp R , <i>E. coli</i> cloning vector	Invitrogen
pMD19-T-hipAB	Amp R , expressing hipAB with its native promoter	This study
pXis $_{21}$	Cm R , expression plasmid for Xis $_{21}$ from GI21	This study
pXis $_{PO1}$	Cm R , expression plasmid for Xis $_{PO1}$ from GISpuPO1	This study
pXis $_{ANA3}$	Cm R , expression plasmid for Xis $_{ANA3}$ from GISspANA3	This study
pInt $_{48}$	Cm R , expression plasmid for Int $_{48}$	This study
pHGI01	Kan R , Integrative lacZ reporter plasmid	Fu et al., 2014
pInt2894	Cm R , expression plasmid for Sputcn32_2894	This study
pHGI01-P $_{int}$	pHGI01 containing 213bp upstream of <i>int</i> (Sputcn32_2900)	This study
pHGR01	Kan R , replicative lacZ reporter plasmid	Fu et al., 2014
pHGR01-P $_{hipA}$	Fuse hipAB promoter from CN32 with lacZ in pHGR01	This study
pK18mobsacB-Cm	Km R , Cm R , SacB, and suicide plasmid used for gene knockout	Wang et al., 2015
pK18Cm-hipAB	pK18mobsacB-Cm containing the homologous arms of hipAB	This study

^aCm R , chloramphenicol resistance; Kan R , kanamycin resistance; and Amp R , ampicillin resistance.

Construction of Plasmids

The primers used in this study are listed in Table 2. The encoding regions of xis $_{21}$, xis $_{PO1}$, xis $_{ANA3}$, int $_{48}$, and int2894 were amplified from the original bacterial host and cloned into the EcoRI and BamHI sites of pHGECm using T4 ligase, generating pXis $_{21}$, pXis $_{PO1}$, pXis $_{ANA3}$, and pInt $_{48}$. The encoding regions of hipA, hipB, and hipAB were amplified

from CN32 and inserted into the *SalI* and *PstI* sites of pCA24N, generating pHipA, pHipB, and pHipAB. The promoter and encoding region of *hipAB* was amplified from CN32 and inserted into pMD19-T, generating pMD19-T-*hipAB*. To construct the *lacZ* reporter plasmid pHGI01-P_{int}, the reporter region of the integrase gene *Sputcn32_2900* was amplified with the primer pair pHGI01-P_{int}-F/-R and fused with the *lacZ* gene in pHGI01. Then, the integrative plasmid pHGI01-P_{int} was transferred into CN32 and Δ *hipAB* by conjugation and integrated into the promoter region of *Sputcn32_2900*, generating CN32 P_{int}::*lacZ* and Δ *hipAB* P_{int}::*lacZ*. The primer sets mob-F/int-R and Int-F/*lacZ*-R were used to confirm the construct. To construct pHGR01-P_{hipA}, the promoter of *hipAB* was amplified with primers pHGR01-P_{hipA}-F/-R from CN32, and inserted into the promoterless-*lacZ* reporter plasmid pHGR01.

Construction of *hipAB* Deletion Mutant in CN32

The deletion mutant Δ *hipAB* was constructed based on pK18*mobsacB*-Cm as described previously (Wang et al., 2015). Briefly, the upstream and downstream regions of *hipAB* were amplified from CN32 using the primers listed in Table 2 and inserted into pK18*mobsacB*-Cm using T4 ligase, producing pK18Cm-*hipAB*. Then, pK18Cm-*hipAB* was introduced into CN32 by conjugation. After mating, cells were spread on LB plates containing Cm to screen the single crossover mutant in which pK18Cm-*hipAB* had integrated into the CN32 genome. The mutant was then grown on LB medium without antibiotics for 8 h. To select mutants in which the second recombination had occurred, the culture was diluted, spread on LB medium containing 10% sucrose, and grown at 30°C for 24–36 h. Single colonies were transferred onto LB- and LB-containing Cm plates simultaneously, and colonies sensitive to Cm were collected and confirmed by PCR followed by DNA sequencing.

Conjugation Assays

The plasmids in this study were transferred from *E. coli* WM3064 into *Shewanella* strains by conjugation assays as described previously (Wang et al., 2015). Briefly, equal amounts of donor and recipient cells were mixed and dropped onto LB medium containing DAP. The plates were incubated at 30°C for 6–8 h, and cells were collected from the lawn and streaked on LB medium with antibiotics to select for transconjugants.

Reporter Activity Assay

Specific β -galactosidase activity was determined by monitoring the absorbance at 420 nm using the Miller assay (Miller, 1972). To determine the promoter activity of *hipAB* under overexpression of HipB and HipB-HipA, plasmids pHipB or pHipAB were transformed into the *E. coli* host carrying the reporter plasmid pHGR01-P_{hipA}. Overnight cultures were diluted 1:100 in LB with Kan and Cm and induced with

0.1 mM IPTG at an OD₆₀₀ of 1.0. After induction for 2 h, cells were collected to determine the β -galactosidase activity.

Quantification of the Excision Rate of GI21 and CGI48

For GI21, GISpANA3, GISpuPO1, and CGI48, *attB/gyrB* indicated the excision rate of the target GIs after excision. We conducted real-time quantitative PCR (qPCR) assays to quantify the *attB* of these GIs as previously reported methods (Burrus and Waldor, 2003; Wang et al., 2017). The primers used for the qPCR assays are listed in Table 2, and chromosomal *gyrB* was used as the reference gene. To test the regulation of Xis and Int on the excision of GI21, GISpANA3, GISpuPO1, and CGI48, pXis₂₁⁻, pXis_{PO1}⁻, pXis_{ANA3}⁻, and pInt₄₈-containing strains were induced with 1.0 mM IPTG for 6 h at an OD₆₀₀ of 0.8–1.

Calculation of % CGI48- and GI21-Free Cells

Both CGI48 and GI21 are non-replicable, and loss of CGI48 and GI21 only occurs after their excision. Therefore, to visualize the loss of CGI48 and GI21, the wild-type and Δ *hipAB* strains carrying pXis₂₁ or pInt₄₈ were induced with 1 mM IPTG for 6 h to overproduce Xis₂₁ (to induce GI21 excision) or Int₄₈ (to induce CGI48 excision). Then, the cells were plated on LB plates containing X-gal to calculate the numbers of white colonies (losing CGI48 or GI21) plus blue colonies, and the white colonies were also confirmed by PCR assay.

Plasmid Stability Assay

The contribution of HipA/HipB TA system to plasmid stability was tested as described previously (Yao et al., 2015). Overnight cultures of *E. coli* BW25113 containing plasmid pHipAB or empty vector pCA24N were grown in LB medium with Cm. Then, the preculture was used to inoculate 3 ml LB without antibiotics. Every 12 h of growth, bacterial suspensions were diluted 1,000-fold in 3 ml fresh LB medium. The cultures were serially diluted in 10-fold dilution steps from 0 to 108 h, and 10 μ l was dropped on LB plates with or without Cm. The colony-forming unit (CFU) assay was conducted every 12 h for 108 h, and the number of CFUs was determined. Each experiment was performed in triplicate with two independent cultures.

RESULTS

CGI48 Is a Composite Island Containing GI21

Comparing the genome sequence of *S. putrefaciens* CN32 with the related strain *S. putrefaciens* W3-18-1, a large region within 3,340,000–3,400,000 of CN32 was absent in the same gene locus (1,160,000–1,170,000) of W3-18-1 (Figure 1A), suggesting that this region was acquired horizontally. Moreover,

TABLE 2 | Primers used in this study.

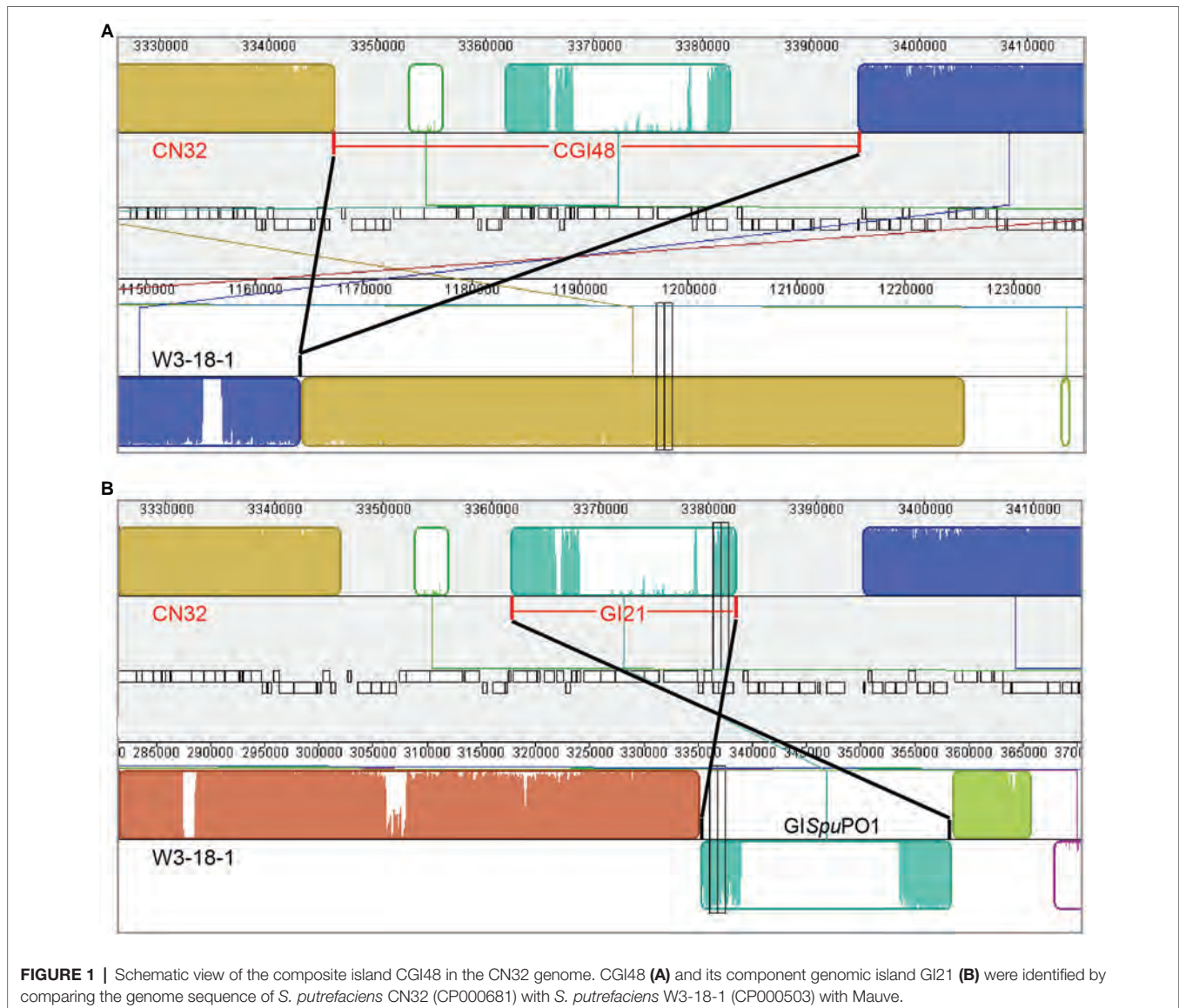
Primers	Sequence (5'-3')	Purpose
Plasmid construction		
Int48-F	CCGGAATTCATGGGTAGTATTAACCTCTCG	pInt ₄₈
Int48-R	CGCGGATCCCTTATCCTCTTAGTTTTGGTTC	
Xis21-F	CCGGAATTCATGAACCCATCAAATCACG	pXis ₂₁
Xis21-R	CGCGGATCCCTAATTGATACTTTTCGCGG	
Int2894-F	CCGGAATTCCTTGTCTAAGGACTCGACGGAG	pInt2894
Int2894-R	CGCGGATCCCTTATTTGTTGTTTCATCATTATTCC	
Xis _{PO1} -F	CCGGAATTCGTGAACATGAACCCATCAAATC	pXis _{PO1}
Xis _{PO1} -R	CGCGGATCCCTAATTGATACTTTTCGCGGTTGG	
Xis _{ANA3} -F	CCGGAATTCGTGAGCATGAACCTATTAATAAAC	pXis _{ANA3}
Xis _{ANA3} -R	CGCGGATCCCTTAGTACTTCCATCTTCGACTG	
hipA-Sall-F	ACGCGTCCGACGAACAGTTGACCATTCAGGC	pHipA
hipA-PstI-R	TGCACTGCGAGTGCATACCAATCCCCAAGCGG	
hipB-Sall-F	ACGCGTCCGACAGTGATAAAACAAACGACTAC	pHipB
hipB-PstI-R	TGCACTGCGAGTGCATAAAAGCCATGTGACAC	
hipA-Sall-F	ACGCGTCCGACGAACAGTTGACCATTCAGGC	pHipAB
hipB-PstI-R	TGCACTGCGAGTGCATAAAAGCCATGTGACAC	
pHGR01-P _{hipA} -F	CCGGAATTCAGTGTAGCGCATATTAATAA	pHGR01-P _{hipA}
pHGR01-P _{hipA} -R	CGCGGATCCgtaatacatggTCATGAAAGCTCCCAAAGACATTATG	
pMD19-T-hipAB-F	TCATAAAAGCCATGTGACAC	pMD19-T-hipAB
pMD19-T-hipAB-R	GTCACCACATTAGTCCCACT	
Construction of Δ hipAB		
hipAB-up-F	ACATGCATGCGAGATGAAACGCTTCAACTCG	pK18Cm-hipAB
hipAB-up-R	CCGGAATTCAGTGGATAGCATTGACCAAC	
hipAB-down-F	CCGGAATTCGCTCGTAATCTAACGAGGTAAG	
hipAB-down-R	AGCGTCCGACCCAGGTTACTAATTCTAGTCAC	
hipAB-wF	GTTTACATAAACACGACGAC	Confirmation of Δ hipAB
hipAB-wR	GTCCATATTACTCACCTTAGC	
Construction of Δ hipAB P _{int} ::lacZ and CN32 P _{int} ::lacZ		
pHG101-P _{int} -F	CCGGAATTC AACGTCGAATGACGTTTTTAGCG	pHG101-P _{int}
pHG101-P _{int} -R	CGCGGATCCgtaatacatggGTAGTTAAAGTCCAAATGGTGAC	
mob-F	CAGAGCAGGATCCCGTTGAGCA	Confirmation of Δ hipAB P _{int} ::lacZ and CN32 P _{int} ::lacZ
LacZ-R	TATTACGCCAGCTGGCGAAAGG	
Int-F	ATGATTAAGTGCACCTTTTCAAGG	
Int-R	CATTTGGCTGCGATTAGCTC	
Primers used in determination of the excision and circled form of CGI48 and GI21		
21F	CCAAAGCGAGGTAAGACGT	Δ GI21
21R	TCGGAGACAGCGATGTATCG	
21cirF	AGTGGGACTAATGTGGTGACTAGAATT	The circled GI21
21cirR	TGCAAGTGCATGGTTTTATGATG	
48F	CCAAGTGAACGTTTATGATCGC	Δ CGI48
48R	GGTGTGTTTTTCATCGTTATGC	
48cirF	CGAGAGTCTATTGCTAGAGAC	The circled CGI48
48cirR	AGAATATGGTCTAACCAAGC	
oF	CCGGAATTCATGATTAAGTGTCACTTTTCAAGG	<i>cro/cl</i> gene
oR	CGCGGATCCCTTAGTCTGTACCTTGGATTTC	
Primers used in qPCR for CGI48 and GI21 in CN32		
q48F	GGCTCGCATATTTCTGTGCAA	Determine the excision rate of CGI48
q48R	CCTTTGAGAGTGCTTTTAGCATAATG	
q21F	TTGGCGAGTTGCTCGAAATC	Determine the excision rate of GI21
q21R	GGAAGTGGGATGTGTTTTATTGC	
q48cF	CGAGAGTCTATTGCTAGAGAC	Determine the circular form of CGI48
q48cR	AGAATATGGTCTAACCAAGC	
q21cF	AGTGGGACTAATGTGGTGACTAGAATT	Determine the circular form of GI21
q21cR	TGCAAGTGCATGGTTTTATGATG	
CN32gyrB-qF	TTCTGACTTTGCTGTTGACCTTCT	Reference gene
CN32gyrB-qR	CTACGGTGCCATCCAATGCT	
Primers used in qPCR for GlSpuPO1 in W3-18-1		
GlSpuPO1-qF	AGGTCGCCGCTCAGATTTTA	Determine the excision rate of GlSpuPO1
GlSpuPO1-qR	TGAGTCGGAACATCATTAGACGTT	

(Continued)

TABLE 2 | Continued

Primers	Sequence (5'-3')	Purpose
W3181gyrB-qF	GCTCAGCCGCCTTTGTTTAA	Reference gene
W3181gyrB-qR	CGGCTCACCCGACATACC	
Primers used in qPCR for <i>GISpANA3</i> in ANA-3		
<i>GISpANA3</i> -qF	GTCGAGCTCAAAGTACTCATCGAA	Determine the excision rate of <i>GISpANA3</i>
<i>GISpANA3</i> -qR	GCTACAGCAGAAGCTAATCTCATTACTC	
ANA3gyrB-qF	CTGGTGAGCCTGTGCTCGAT	Reference gene
ANA3gyrB-qR	CAAGCGCCGCACCTAACTTA	

Restriction sites included in oligonucleotide sequences are underlined.



the internal sequence within 3,360,000–3,380,000 of this large region showed high homology with another region 335,000–360,000 of W3-18-1 (Figure 1B). These results suggested that the region within 3,340,000–3,400,000 of CN32

is a putative composite genomic island. It is 48 kb in length; thus, it is designated CGI48 hereafter (Table 3). Further analysis showed that region 3,360,000–3,380,000 of CN32 contains a 21 kb genomic island (designated GI21), which

TABLE 3 | Sequence analysis of composite island CGI48.

Gene	Start	End	Strand	Functions
<i>attL</i> ₄₈	3,346,221	3,346,273	+	Left attachment site of CGI48
Sputcn32_2886	3,346,726	3,347,073	+	Hypothetical protein
Sputcn32_2887	3,347,409	3,347,561	+	Pseudo
Sputcn32_2888	3,348,921	3,347,632	–	Beta-lactamase domain protein
Sputcn32_2889	3,349,853	3,348,921	–	Hypothetical protein
Sputcn32_2890	3,350,524	3,349,859	–	Metallophosphoesterase
Sputcn32_2891	3,351,168	3,350,566	–	Conserved hypothetical protein
Sputcn32_2892	3,351,518	3,352,093	+	Hypothetical protein
Sputcn32_2893	3,352,083	3,354,299	+	Hypothetical protein
Sputcn32_2894	3,354,292	3,357,321	+	Phage integrase
Sputcn32_2895	3,357,533	3,358,846	+	Conserved hypothetical protein
Sputcn32_2896	3,359,598	3,359,224	–	Conserved hypothetical protein
Int ₄₈ , Sputcn32_2897	3,361,269	3,360,109	–	Phage integrase
Sputcn32_2898	3,361,484	3,361,278	–	Transcription-repair coupling factor (superfamily II helicase)
Sputcn32_2899	3,361,613	3,361,819	+	Predicted transcriptional regulator, Cro/Ci family
<i>attL</i> ₂₁	3,361,829	3,361,837	+	Left attachment site of GI21
Sputcn32_2900 ^a	3,362,021	3,363,319	+	Phage Integrase
Sputcn32_2901 ^a	3,363,329	3,364,162	+	Hypothetical protein
Xis ₂₁ , Sputcn32_2902 ^a	3,364,278	3,364,487	+	AlpA family phage transcriptional regulator
Sputcn32_2903 ^a	3,364,910	3,365,845	+	Hypothetical protein
Sputcn32_2904 ^a	3,366,023	3,366,676	+	Conserved hypothetical protein
Sputcn32_2905 ^a	3,367,222	3,366,839	–	Hypothetical protein
Sputcn32_2906 ^a	3,367,382	3,367,798	+	Putative DNA-binding protein
Sputcn32_2907 ^a	3,367,890	3,368,189	+	Protein of unknown function UPF0150
Sputcn32_2908 ^a	3,368,533	3,370,104	+	Type I restriction-modification system, M subunit, N-6 DNA methylase
Sputcn32_2909 ^a	3,370,094	3,371,416	+	Type I restriction-modification system, specificity subunit S (EC 3.1.21.3)
Sputcn32_2910 ^a	3,371,431	3,374,133	+	ATPase associated with various cellular activities, AAA_5 ⁷
Sputcn32_2911 ^a	3,374,133	3,375,440	+	Conserved hypothetical protein
Sputcn32_2912 ^a	3,375,839	3,378,976	+	Type I restriction-modification system, restriction subunit R (EC 3.1.21.3)
Sputcn32_2913 ^a	3,379,461	3,379,039	–	Transcriptional regulator, XRE family
Sputcn32_2914 ^a	3,379,625	3,380,281	+	Conserved hypothetical protein
HipB, Sputcn32_2915 ^a	3,380,923	3,380,465	–	Transcriptional regulator, XRE family
HipA, Sputcn32_2916 ^a	3,382,266	3,380,920	–	HipA domain protein
<i>attR</i> ₂₁	3,382,740	3,382,748	+	Right attachment site of GI21
Sputcn32_2917	3,383,263	3,383,625	+	Conserved hypothetical protein
Sputcn32_2918	3,384,571	3,383,654	–	Transposase, IS4 family
Sputcn32_2919	3,385,229	3,384,696	–	Conserved hypothetical protein
Sputcn32_2,920	3,386,826	3,385,240	–	Von Willebrand factor, type A
Sputcn32_2921	3,388,288	3,386,819	–	ATPase associated with various cellular activities, AAA_5
Sputcn32_2922	3,389,920	3,388,445	–	Sigma54 specific transcriptional regulator, Fis family
Sputcn32_2923	3,390,290	3,390,066	–	Hypothetical protein
Sputcn32_2924	3,390,847	3,390,707	–	Pseudo
Sputcn32_2925	3,392,615	3,390,858	–	Methyltransferase type 11
Sputcn32_2926	3,393,959	3,393,004	–	Pseudo
Sputcn32_2927	3,394,306	3,394,382	+	tRNA-Trp
<i>attR</i> ₄₈	3,394,303	3,394,355	–	Right attachment site of CGI48

^aThe genes in GI21.

exhibits sequence identity with genomic islands integrated in the conserved *yicC* gene, such as GISpuPO1 in *S. putrefaciens* W3-18-1, GISpANA3 in *Shewanella* sp. ANA-3, and GIPspSM9913 in *Pseudoalteromonas* sp. SM9913 (**Figure 2A**). GI21 exhibits 99% sequence identity with the two ends of GISpuPO1 in W3-18-1. The left region of GI21 contains an integrase and an excisionase gene next to the left attachment site (*attL*₂₁), and the right region contains a putative *hipA-hipB* toxin–antitoxin pair next to the right attachment site (*attR*₂₁). The middle region contains 12 genes encoding a restriction–modification system and hypothetical proteins (**Figure 2A**).

Excision of GI followed by formation of circular forms of GI is prerequisite for its horizontal transfer. Integrase is essential for GI excision and integration, and some GIs also encode recombination directionality factors (or excisionases Xis) directing the reaction toward excision (Lewis and Hatfull, 2001). We wondered whether GI21 can be excised from the CGI48 genome by recombining the attachment *attL*₂₁ and *attR*₂₁, and producing *attB*₂₁ and *attP*₂₁ sites (**Figure 2B**). Quantitative PCR (qPCR) was used to quantify the excision rate by measuring the percentage of cells in the culture containing *attB*₂₁, which is only present after GI21 excision. In this assay, the amount of *attB*₂₁ sites is compared to the

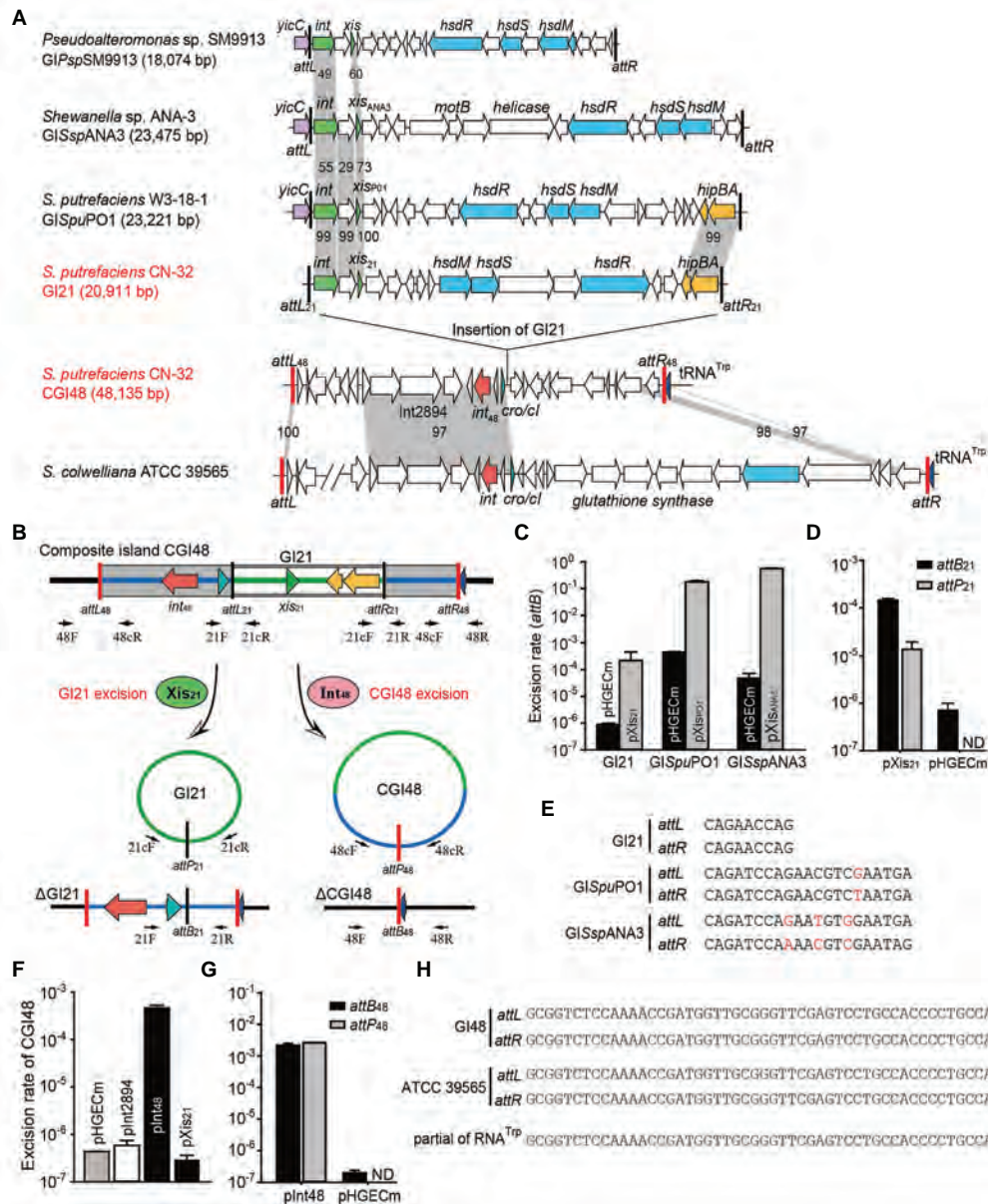


FIGURE 2 | The composite island CGI48 and its component GI21 can be excised from the CN32 genome. **(A)** Sequence analysis of CGI48 with the related genomic islands. Open reading frames with putative functions are shown in different colors. The *attL* and *attR* attachment sites of CGI48 and GI21 are shown in red and black, respectively. The sequence of the GI integrated into tRNA^{Trp} of ATCC 39565 genome was in L876DRAFT_scaffold 00018.18_C (82,217–85,620bp) to scaffold 00033.33_C (1,478–38,068bp). **(B)** Schematic of the excision of CGI48 and GI21. **(C)** The excision rate of GI21, GISpuPO1, and GISspANA3 was quantified when cognate excisionase was overexpressed. **(D)** Comparison of the excision rate (*attB*₂₁) and circular form of GI21 (*attP*₂₁) in CN32 when Xis21 was overexpressed. ND indicates not detected. **(E)** Sequence comparison of the attachments of GI21, GISpuPO1, and GISspANA3. **(F)** The excision rate of CGI48 when Int₄₈ was overexpressed. **(G)** Comparison of the excision rate (*attB*₄₈) and circular form of CGI48 (*attP*₄₈) in CN32 when Int48 was overexpressed. ND indicates not detected. **(H)** Sequence comparison of the attachment sites of CGI48 and GI in ATCC 39565 compared with the 3' end of RNA^{Trp} in *Shewanella*.

amount of the reference gene *gyrB*, which is used to quantify the total number of cells in the culture. Excisionase Sputcn32_2902 (Xis₂₁) was induced in strain CN32 with 1 mM IPTG for 6 h. Additionally, the excisionases Xis_{PO1} and Xis_{ANA3} were also overexpressed in W3-18-1 and ANA-3 as a control. The results showed that Xis₂₁ mediated GI21

excision, resulting in a 440-fold increase in the excision rate of GI21 and reaching $(3.8 \pm 0.3) \times 10^{-4}$. However, the excision rate of GISpuPO1 and GISspANA3 reached 17.9%–55.6% when Xis_{PO1} and Xis_{ANA3} were overexpressed, which was much higher than that of GI21 (Figure 2C). qPCR was also used to quantify the circular form of GI21 by

measuring *attP*₂₁, which is present after GI21 is circularized or replicated after excision. The number of *attP*₂₁ is less than *attB*₂₁, suggesting that GI21 is non-replicable in wild-type CN32 or expressing Xis₂₁ (Figure 2D). PCR sequencing showed that the attachment sites of GISpuPO1 and GISpANA3 were 21 bp in length, and the attachment sites of GI21 were 9 bp (Figure 2E). In CGI48, GI21 was integrated in the untranslated region between *Sputcn32_2899* and *Sputcn32_2917*, which encoded a predicted transcriptional regulator of the Cro/CI family and a conserved hypothetical protein, respectively (Figure 2A). The excision and integration of GI21 did not cause any sequence changes in the neighboring genes. The results suggested that GI21 can be excised from CN32 by site-specific recombination of *attL*₂₁ and *attR*₂₁, and the shorter attachment sites may greatly limit the recombination efficiency.

We then evaluated the excision of CGI48 (Figure 2B), and the integrase genes *Sputcn32_2894* and *Sputcn32_2897* were cloned into pHGECm for their overexpression. Overproduction of *Sputcn32_2897* (named Int₄₈) resulted in a 1.070-fold increase in the excision rate of CGI48 and reached $(4.7 \pm 0.6) \times 10^{-4}$, and *Sputcn32_2894* did not affect the excision of CGI48 (Figure 2F). Quantification of *attP*₄₈ indicated that CGI48 is non-replicable in wild-type CN32 or expressing Int₄₈ (Figure 2G). Sequence analysis showed that CGI48 was integrated in the 5' end of tRNA^{Trp}, a conserved integration locus of GIs, such as the GI in *S. colwelliana* ATCC 39565 (Figure 2A). PCR sequencing confirmed that CGI48 and GI in *S. colwelliana* ATCC 39565 shared 100% identical attachment sites of 50 bp in length, and the excision and integration did not cause sequence changes in tRNA^{Trp} (Figure 2H). Phylogenetic tree analysis of Int₂₁ and Int₄₈ revealed that GI21 homologs are widely distributed in *Shewanella*, *Pseudoalteromonas*, *Halomonas*, and *Vibrio* strains (Figure 3A), and CGI48 homologs are widely distributed in *Shewanella*, *Pseudomonas*, *Halomonas*, and *Photobacterium* strains (Figure 3B). Collectively, CGI48 and the component GI21 can be excised from the CN32 genome, suggesting that CGI48 is an active composite island in host bacteria.

GI21 Encodes a HipAB Toxin–Antitoxin System

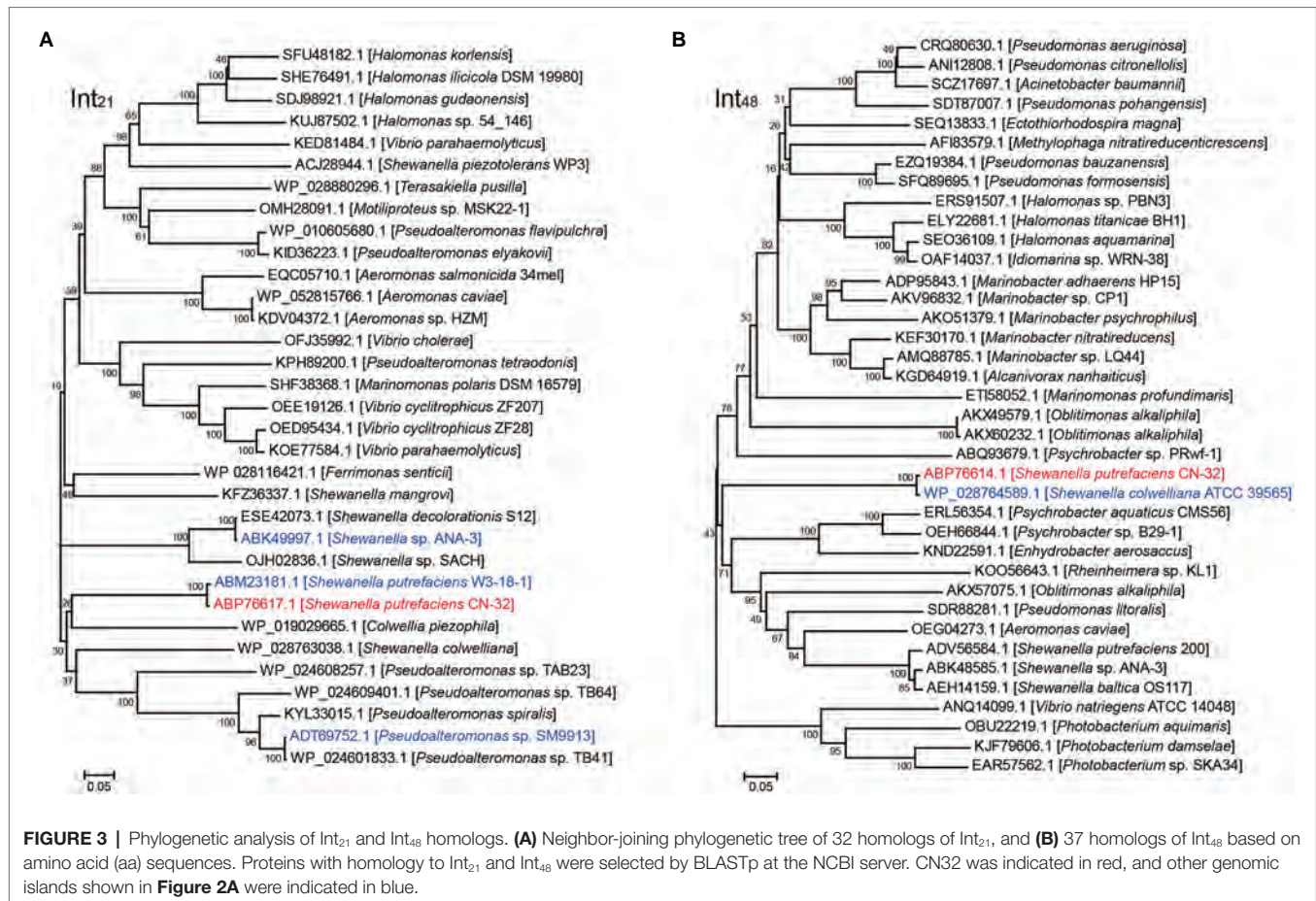
In GI21, two neighboring genes that are only 4 bp apart, *Sputcn32_2916* and *Sputcn32_2915*, were identified as a putative *hipA-hipB* TA pair. In HipA/HipB TA system characterized in *E. coli* K-12, HipA_{K-12} toxin functions as a serine/threonine protein kinase that inhibits cell growth, and HipB_{K-12} antitoxin encoded by the gene upstream to *hipA* blocks its effects (Germain et al., 2013). Here, the putative *hipA-hipB* TA pair in GI21 has a genetic architecture reversed to that of *hipB-HipA* in *E. coli* K-12 (Figure 4A). *Sputcn32_2916* encodes a HipA domain protein that is 448 aa in length, and it has 40% identity and 6% coverage with HipA_{K-12}. *Sputcn32_2915* encodes a XRE family transcriptional regulator of 152 aa that contains a Helix-turn-helix (HTH)

domain in the C-terminal and has 33% amino acid sequence identity and 23% coverage with HipB_{K-12} (Figure 4B). To determine whether *Sputcn32_2916* and *Sputcn32_2915* constitute a functional TA pair, open reading frames of the two genes were cloned into plasmid pCA24N to obtain pHipA and pHipB, respectively. Expression of *hipA* or *hipB* was induced in *E. coli* BW25113 with 0.5 mM IPTG. Cell growth (turbidity) and cell viability (CFU ml⁻¹) were measured for 8 h. Overproducing HipA in BW25113 cells led to growth inhibition (Figures 4C–E). To further assess whether HipB can block the toxicity of HipA, we cloned the coding regions of *hipA* and *hipB* into plasmid pCA24N to construct pHipAB. Coexpression of *hipA* and *hipB* via plasmid pHipAB in BW25113 cells showed that HipB could partially neutralize the toxic effect of HipA (Figures 4C–E); this may result from the too high load of toxins driven by the strong *lac* promoter on the high copy number plasmid pCA24N. Then, we cloned *hipA-hipB* with its native promoter into pMD19-T to generate pMD19-T-*hipAB*. The strain BW25113/pMD19-T-*hipAB* exhibited similar cell viability with that of BW25113/pMD19-T, suggesting that HipB could fully neutralize the toxic effect of HipA under the native promoter (Figure 4F). Taken together, HipA and HipB in GI21 form a TA pair in which HipA is a potent toxin and HipB is the cognate antitoxin.

In HipA_{K-12}/HipB_{K-12}, the antitoxin HipB_{K-12} or the TA complex bind DNA and autoregulate the transcription of the TA operon (Black et al., 1994). Similar to HipB_{K-12}, HipB in CN32 also contains a HTH domain, thus we wondered whether HipB in GI21 can regulate the *hipA-hipB* operon. Using the plasmid by fusing *lacZ* with the *hipA-hipB* promoter as the reporter, we found that overproduction of HipB exhibited 2.1 ± 0.1-fold decrease in the promoter activity compared to empty vector. Moreover, overproduction of HipA/HipB complex via pHipAB showed a 2.9 ± 0.4-fold decrease in the promoter activity (Figure 4G). These results suggested that GI21-encoded HipB and the HipA/HipB complex can repress the TA operon.

GI21-Encode HipAB Stabilizes CGI48

To test whether the HipA/HipB TA system affects the excision of CGI48, we deleted the *hipAB* region in CN32. qPCR assays showed no significant difference in the excision rate of CGI48 in the *hipAB* deletion mutant compared to wild-type CN32 (Figure 5A). As reported in our previous study, the TA system in prophage CP4So in *S. oneidensis* stabilizes CP4So after its excision (Yao et al., 2018). We wondered whether GI21-encoding HipA/HipB played a role in the maintenance of CGI48 after its excision. A blue–white reporter screening assay was designed to detect the loss of GI21 and CGI48 after their excision. In brief, the *lacZ* gene was fused with the promoter of the integrase gene *Sputcn32_2900* to generate a P_{int}::*lacZ* fusion and cloned into the integrative plasmid pHGI01, generating pHGI01-P_{int}. The constructed plasmid was site specifically integrated into GI21 in CN32. Blue colonies indicated the presence of GI21 in CN32, irrespective of whether it was integrated in the host



chromosome or existed in a circular form after GI21 or CGI48 was excised. White colonies indicated a complete loss of GI21 from CGI48 or a complete loss of CGI48 from the CN32 genome (**Figure 5B**). To activate the excision of GI21 and CGI48, *Xis*₂₁ and *Int*₄₈ were induced with 1 mM IPTG for 6 h, and cells were then plated on X-gal plates to detect GI21- and CGI48-free cells using the reporter plasmid (**Figure 5C**). No loss of GI21 was detected in wild-type CN32, and 0.39% of GI21-free cells were exhibited in the *hipAB* deletion mutant when *Xis*₂₁ was overexpressed. Similarly, no loss of CGI48 was detected in wild-type CN32, and 0.82% of CGI48-free cells was exhibited in the *hipAB* deletion mutant when *Int*₄₈ was overexpressed (**Figure 5D**). Then, two white colonies (indicated with blue arrows) from the *Xis*₂₁-induced plates and two (indicated with blue arrows) from the *Int*₄₈-induced plates were randomly selected to confirm the loss of GI21 and CGI48 (**Figure 5E**) by PCR. In addition, we also test the contribution of GI21-encoded HipA/HipB on plasmid stability. As shown in **Figure 5F**, plasmid pCA24N was completely lost from *E. coli* BW25113 after 72 h, while pHipAB which contains *hipAB* in pCA24N was stably maintained in *E. coli* after 108 h of culturing. Altogether, these results thus demonstrate that HipA/HipB not only stabilizes GI21 and CGI48 but also provides plasmid stabilization.

CONCLUSION AND DISCUSSION

In this study, a new composite island, CGI48, was detected in the genome of *S. putrefaciens* CN-32. CGI48 harbors genes encoding adaptive traits, such as antibiotics and restriction–modification systems. CGI48 evolved by inserting a genomic island, GI21, showing high identity with GIs integrated in the *yicC* locus. Because the conserved *yicC* locus is intact and available in CN32 genome, GI21 might integrated into CN32 accompanied by the composite CGI48. Another possibility is that GI21 is integrated into the secondary attachment site within CGI48 genome after horizontal gene transfer. Many genomic islands preferentially integrated into a primary attachment site in the bacterial genome. Studies on the ICEs, ICEBs1 found that ICEBs1 can also integrate into secondary attachment site, especially when the primary site is absent. However, the excision of ICEBs1 from secondary sites is greatly reduced compared to the primary site, limiting the dissemination of ICEBs1 (Menard and Grossman, 2013). *In vitro* assays showed that the efficiency of integrase-mediated site-specific recombination is related to the length of the attachment site, and the reduction of the core attachment site produced a dramatically decrease in the recombination activity (Ghosh et al., 2003). Thus, we speculated that the shorter attachment sites flanking GI21 may limit its excision

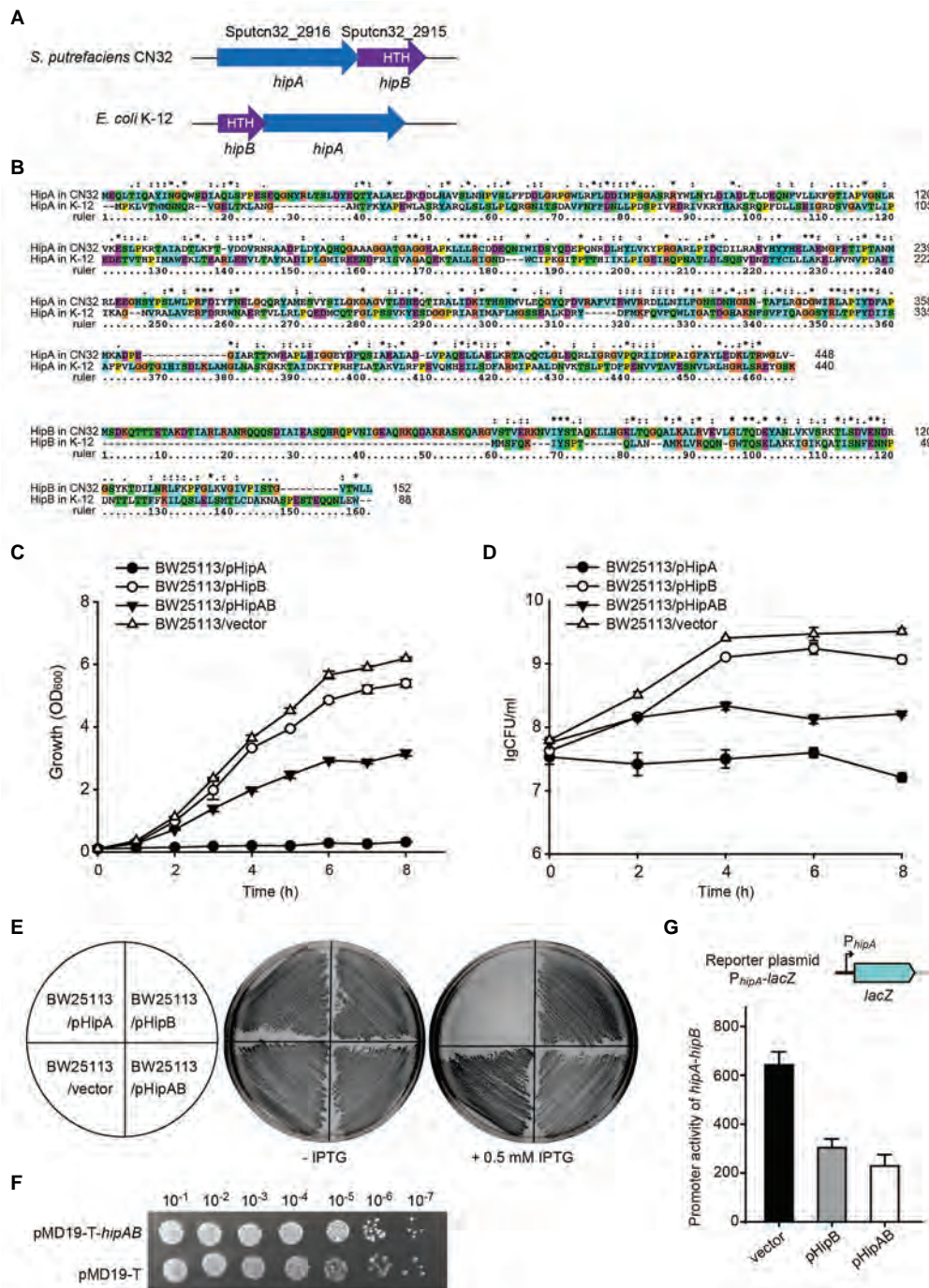


FIGURE 4 | HipA and HipB in Gl21 constitute a Toxin–antitoxin (TA) pair. **(A)** Comparison of the *hipA-hipB* operon in Gl21 and *hipB-hipA* operon in *E. coli* K-12. **(B)** Sequence alignment was carried out using ClustalX to compare the amino acid sequence identity of HipA/HipB in *S. putrefaciens* CN32 and *E. coli* K-12. Cell growth **(C)** and cell viability **(D)** of cells overexpressing *hipA*, *hipB*, and *hipA-hipB* via pCA24N-based plasmids in *E. coli* BW25113. **(E)** Growth of BW25113 cells overexpressing *hipA*, *hipB*, and *hipA-hipB* via pCA24N-based plasmids on LB plates with and without 0.5 mM isopropyl- β -D-thiogalactopyranoside (IPTG). **(F)** CFU of strain BW25113 containing pMD19-T-*hipAB* or empty vector pMD19-T on LB plates with ampicillin. **(G)** The activity of the *hipA-hipB* promoter in Gl21 was measured by overexpressing *hipB* or *hipA-hipB*.

and stabilize the composite structure. Some composite GIs are also found to be stabilized by truncated attachment sites or integrases (Bellanger et al., 2014). In this study, we also

found that a functional TA system maintain the stability of the composite GI. All these mechanisms explain the complexity and diversity of GIs.

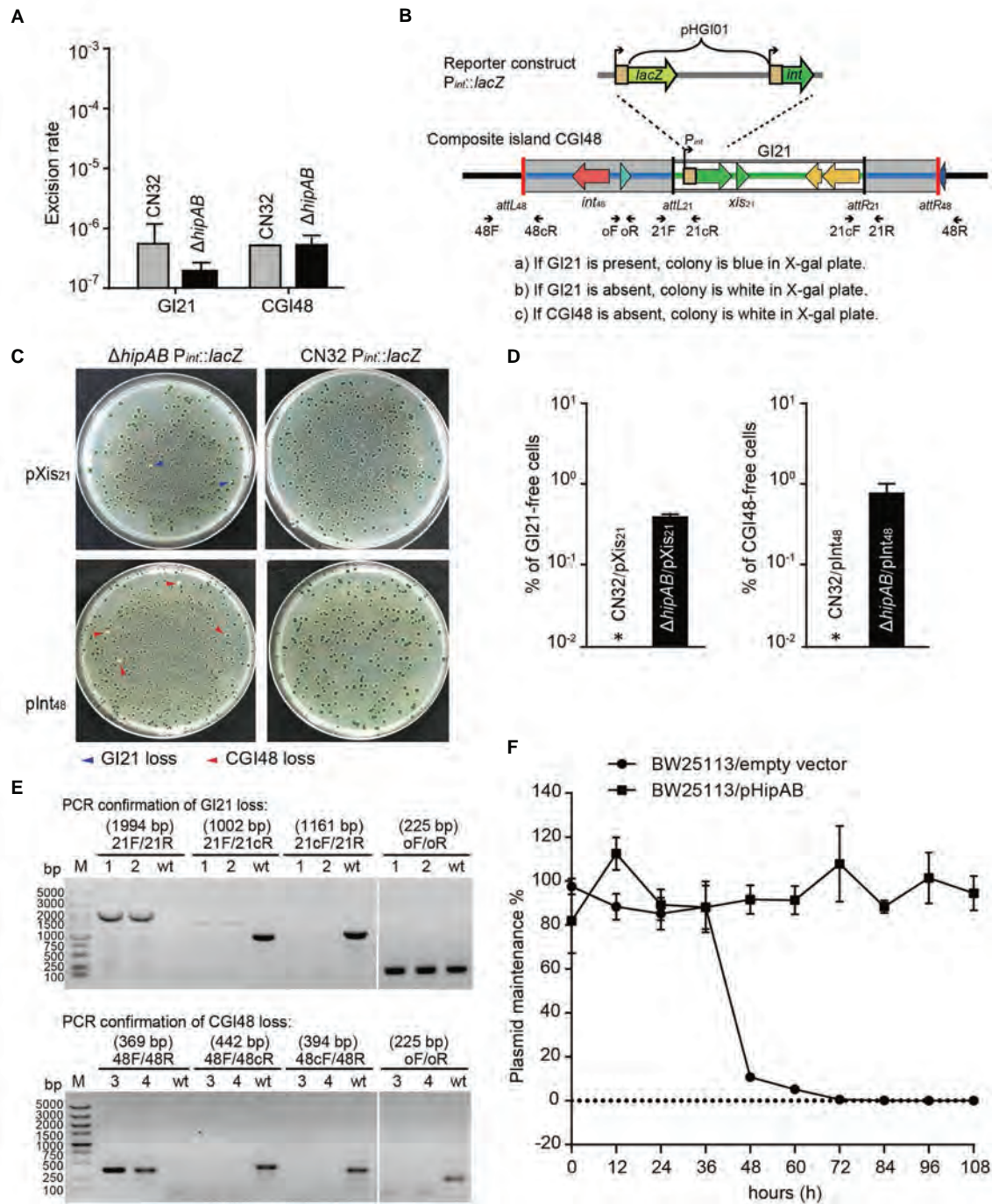


FIGURE 5 | GI21-encoded HipAB promotes the maintenance of CGI48. **(A)** The excision rate of GI21 and CGI48 in the CN32 wild-type and $\Delta hipAB$ mutant strains. **(B)** Schematic of the *lacZ* reporter constructs in the CN32 wild-type and $\Delta hipAB$ strains. **(C)** Observation of GI21 loss when *Xis*₂₁ is overexpressed (upper plates) and of CGI48 loss when *Int*₄₈ is overexpressed (lower plates) on X-gal plates using the *lacZ* reporter system. **(D)** % of GI21-free cells (left panel) and % CGI48-free cells (right panel) were quantified by counting five plates, a representative image as shown in **(C)**. Asterisks indicate that the frequency of GI21 and CGI48 loss was below the limit of detection of the assays ($<1 \times 10^{-5}$). **(E)** Confirmation of GI21 (upper panel) and CGI48 (lower panel) loss by PCR using the indicated primers in **(B)**. 1 and 2 indicate the DNA templates extracted from the colonies with blue arrows in **(C)**; 3 and 4 indicate the DNA templates extracted from the colonies with red arrows in **(C)**; wt indicates the DNA templates from wild-type CN32 used as a control. Lane M indicates DNA Marker DL5k. The expected product sizes are indicated at the top of the primer sets. **(F)** GI21-encoded HipAB confers plasmid stability in *E. coli*. *E. coli* BW25113 harboring plasmids pHipAB and empty vector pCA24N were used in this assay. Three independent cultures were conducted, and the data are shown as means \pm SDs.

DATA AVAILABILITY STATEMENT

The datasets presented in this study can be found in online repositories. The names of the repository/repositories and accession number(s) can be found at: <https://www.ncbi.nlm.nih.gov/genbank/>, CP000503; <https://www.ncbi.nlm.nih.gov/genbank/>, CP000681.

AUTHOR CONTRIBUTIONS

XW and PW conceptualized and designed the project. YZ, WW, JY, XW, DL, and PW did the investigation, data curation, and analysis. YZ, XW, DL, and PW wrote, reviewed, and edited the original draft. All authors contributed to the article and approved the submitted version.

REFERENCES

- Baba, T., Ara, T., Hasegawa, M., Takai, Y., Okumura, Y., Baba, M., et al. (2006). Construction of *Escherichia coli* K-12 in-frame, single-gene knockout mutants: the Keio collection. *Mol. Syst. Biol.* 2:2006.0008. doi: 10.1038/msb4100050
- Bellanger, X., Payot, S., Leblond-Bourget, N., and Guedon, G. (2014). Conjugative and mobilizable genomic islands in bacteria: evolution and diversity. *FEMS Microbiol. Rev.* 38, 720–760. doi: 10.1111/1574-6976.12058
- Black, D. S., Irwin, B., and Moyed, H. S. (1994). Autoregulation of *hip*, an operon that affects lethality due to inhibition of peptidoglycan or DNA synthesis. *J. Bacteriol.* 176, 4081–4091. doi: 10.1128/jb.176.13.4081-4091.1994
- Burrus, V., Roussel, Y., Decaris, B., and Guedon, G. (2000). Characterization of a novel integrative element, ICE*St1*, in the lactic acid bacterium *Streptococcus thermophilus*. *Appl. Environ. Microbiol.* 66, 1749–1753. doi: 10.1128/AEM.66.4.1749-1753.2000
- Burrus, V., and Waldor, M. K. (2003). Control of SXT integration and excision. *J. Bacteriol.* 185, 5045–5054. doi: 10.1128/JB.185.17.5045-5054.2003
- Caro-Quintero, A., Deng, J., Auchtung, J., Brettar, L., Hofle, M. G., Klappenbach, J., et al. (2011). Unprecedented levels of horizontal gene transfer among spatially co-occurring *Shewanella* bacteria from the Baltic Sea. *ISME J.* 5, 131–140. doi: 10.1038/ismej.2010.93
- Dehio, C., and Meyer, M. (1997). Maintenance of broad-host-range incompatibility group P and group Q plasmids and transposition of Tn5 in *Bartonella henselae* following conjugal plasmid transfer from *Escherichia coli*. *J. Bacteriol.* 179, 538–540. doi: 10.1128/jb.179.2.538-540.1997
- Dobrindt, U., Hochhut, B., Hentschel, U., and Hacker, J. (2004). Genomic islands in pathogenic and environmental microorganisms. *Nat. Rev. Microbiol.* 2, 414–424. doi: 10.1038/nrmicro884
- Fu, H., Jin, M., Ju, L., Mao, Y., and Gao, H. (2014). Evidence for function overlapping of CymA and the cytochrome *bc₁* complex in the *Shewanella oneidensis* nitrate and nitrite respiration. *Environ. Microbiol.* 16, 3181–3195. doi: 10.1111/1462-2920.12457
- Germain, E., Castro-Roa, D., Zenkin, N., and Gerdes, K. (2013). Molecular mechanism of bacterial persistence by HipA. *Mol. Cell* 52, 248–254. doi: 10.1016/j.molcel.2013.08.045
- Ghosh, P., Kim, A. I., and Hatfull, G. F. (2003). The orientation of mycobacteriophage Bxb1 integration is solely dependent on the central dinucleotide of *attP* and *attB*. *Mol. Cell* 12, 1101–1111. doi: 10.1016/s1097-2765(03)00444-1
- Haskett, T. L., Terpolilli, J. J., Bekuma, A., O'hara, G. W., Sullivan, J. T., Wang, P., et al. (2016). Assembly and transfer of tripartite integrative and conjugative genetic elements. *Proc. Natl. Acad. Sci. U. S. A.* 113, 12268–12273. doi: 10.1073/pnas.1613358113
- Jurenas, D., Fraikin, N., Goormaghtigh, F., and Van Melderen, L. (2022). Biology and evolution of bacterial toxin-antitoxin systems. *Nat. Rev. Microbiol.* doi:10.1038/s41579-021-00661-1 [Epub ahead of print].

FUNDING

This work was supported by the Guangdong Major Project of Basic and Applied Basic Research (2019B030302004), the Natural Science Foundation of Guangdong Province (2019A1515011912), the Science and Technology Planning Project of Guangzhou (202002030493), Hainan Provincial Joint Project of Sanya Yazhou Bay Science and Technology City (320LH047), the Youth Innovation Promotion Association CAS (2021345 to PW), the Key Special Project for Introduced Talents Team of Southern Marine Science and Engineering Guangdong Laboratory (Guangzhou; GML2019ZD0407), the Natural Science Foundation of Hebei Province (C2019205044), Research Fund of Hebei Normal University (L2016Z03), and Science and Technology Research Project of Hebei University (ZD2018070).

- Kitagawa, M., Ara, T., Arifuzzaman, M., Ioka-Nakamichi, T., Inamoto, E., Toyonaga, H., et al. (2005). Complete set of ORF clones of *Escherichia coli* ASKA library (a complete set of *E. coli* K-12 ORF archive): unique resources for biological research. *DNA Res.* 12, 291–299. doi: 10.1093/dnares/dsi012
- Lei, C. W., Zhang, A. Y., Liu, B. H., Wang, H. N., Yang, L. Q., Guan, Z. B., et al. (2015). Two novel *salmonella* genomic island 1 variants in *Proteus mirabilis* isolates from swine farms in China. *Antimicrob. Agents Chemother.* 59, 4336–4338. doi: 10.1128/AAC.00120-15
- Lewis, J. A., and Hatfull, G. F. (2001). Control of directionality in integrase-mediated recombination: examination of recombination directionality factors (RDFs) including Xis and *cox* proteins. *Nucleic Acids Res.* 29, 2205–2216. doi: 10.1093/nar/29.11.2205
- Menard, K. L., and Grossman, A. D. (2013). Selective pressures to maintain attachment site specificity of integrative and conjugative elements. *PLoS Genet.* 9:e1003623. doi: 10.1371/journal.pgen.1003623
- Miller, J.H. (1972). *Experiments in Molecular Genetics*. Cold Spring Harbor, NY: Cold Spring Harbor Laboratory Press
- Ogura, T., and Hiraga, S. (1983). Mini-F plasmid genes that couple host cell division to plasmid proliferation. *Proc. Natl. Acad. Sci. U. S. A.* 80, 4784–4788. doi: 10.1073/pnas.80.15.4784
- Roberts, R. C., Strom, A. R., and Helinski, D. R. (1994). The *parDE* operon of the broad-host-range plasmid RK2 specifies growth inhibition associated with plasmid loss. *J. Mol. Biol.* 237, 35–51. doi: 10.1006/jmbi.1994.1207
- Smyth, D. S., and Robinson, D. A. (2009). Integrative and sequence characteristics of a novel genetic element, ICE*6013*, in *Staphylococcus aureus*. *J. Bacteriol.* 191, 5964–5975. doi: 10.1128/JB.00352-09
- Wang, X., Yao, J., Sun, Y. C., and Wood, T. K. (2021). Type VII toxin/antitoxin classification system for antitoxins that enzymatically neutralize toxins. *Trends Microbiol.* 29, 388–393. doi: 10.1016/j.tim.2020.12.001
- Wang, P., Yu, Z., Li, B., Cai, X., Zeng, Z., Chen, X., et al. (2015). Development of an efficient conjugation-based genetic manipulation system for *Pseudoalteromonas*. *Microb. Cell Factories* 14:11. doi: 10.1186/s12934-015-0194-8
- Wang, P., Zeng, Z., Wang, W., Wen, Z., Li, J., and Wang, X. (2017). Dissemination and loss of a biofilm-related genomic island in marine *Pseudoalteromonas* mediated by integrative and conjugative elements. *Environ. Microbiol.* 19, 4620–4637. doi: 10.1111/1462-2920.13925
- Wozniak, R. A., and Waldor, M. K. (2009). A toxin-antitoxin system promotes the maintenance of an integrative conjugative element. *PLoS Genet.* 5:e1000439. doi: 10.1371/journal.pgen.1000439
- Yao, J., Guo, Y., Wang, P., Zeng, Z., Li, B., Tang, K., et al. (2018). Type II toxin/antitoxin system ParE_{So}/CopA_{So} stabilizes prophage CP4So in *Shewanella oneidensis*. *Environ. Microbiol.* 20, 1224–1239. doi: 10.1111/1462-2920.14068
- Yao, J., Guo, Y., Zeng, Z., Liu, X., Shi, F., and Wang, X. (2015). Identification and characterization of a HEPN-MNT family type II toxin-antitoxin in

Shewanella oneidensis. *Microb. Biotechnol.* 8, 961–973. doi: 10.1111/1751-7915.12294

Conflict of Interest: The authors declare that the research was conducted in the absence of any commercial or financial relationships that could be construed as a potential conflict of interest.

Publisher's Note: All claims expressed in this article are solely those of the authors and do not necessarily represent those of their affiliated organizations, or those of the publisher, the editors and the reviewers. Any product that may

be evaluated in this article, or claim that may be made by its manufacturer, is not guaranteed or endorsed by the publisher.

Copyright © 2022 Zhao, Wang, Yao, Wang, Liu and Wang. This is an open-access article distributed under the terms of the Creative Commons Attribution License (CC BY). The use, distribution or reproduction in other forums is permitted, provided the original author(s) and the copyright owner(s) are credited and that the original publication in this journal is cited, in accordance with accepted academic practice. No use, distribution or reproduction is permitted which does not comply with these terms.